A Virtual Reality Guidance System for a Precise MRI Injection Robot

Waiman Meinhold, Heriberto A. Nieves-Vazquez, Daniel E. Martinez, Joseph Lee, Siyu Li, Jun Ueda, *Senior Member, IEEE*, and Ai-Ping Hu

***Abstract*— A large number of robots have been developed for image-guided interventions, with increased precision and improved control methods enabling procedures involving complicated and sensitive anatomical targets such as the spinal cord. While image-guided controllers are capable of accurate positioning at, or even beyond, the resolution of the chosen imaging device, targets for interventions are often manually selected from the available imaging data. This work involves the development of an intuitive and immersive virtual reality tool for detecting and visualizing scanner image data during the operation of a precision MRI-guided robot. This tool is integrated into the workflow of the image guidance protocol. Automated surgical freedom analysis is performed with the intention of further augmenting the trajectory selection process. A user study gauges both expert and novice reactions to the system.**

MRI, Virtual Reality, Image Guided Surgery, Surgical Freedom

I. Introduction

With the significant advancement of robots for surgical applications, a parallel development of control interfaces has taken place. This work seeks to bridge the gap between a precise Magnetic Resonance Imaging (MRI) guided robot for surgical tool orientation and a visualization interface used for tool trajectory selection. The automated detection and immersive visualization of the robot and target tissues is expected to aid adoption of the robotic system in a wide range of clinical procedures, from precise intraspinal injection of cellular therapeutics to medial branch blocks for back pain and radiofrequency ablation (RFA) or radiofrequency neurotomy (RFN), all of which require precise targeting of highly localized areas [1], [2].

One procedure of particular interest is the injection of cellular therapeutics directly into the spinal cord to treat neurological conditions such as amyotrophic lateral sclerosis (ALS) [3], [1]. This procedure has typically been performed via open surgery, due to difficulty in accessing the small cross sectional region of the ventral horn [3]. More recently, an adjustable frame was used to perform the same procedure under MRI guidance, with a manual iterative positioning procedure [1]. Scanner time limits and strict accuracy requirements led to the development of the robotic device used in this work [4], [5]. In this case, identifying a target needle path between the vertebrae and into the small area of the ventral horn remains the critical challenge, as once the target path is identified, the robot can automatically move to the corresponding configuration [4]. This work introduces a virtual reality (VR) system for detection and visualization of the robot configuration and target tissue in order to address this challenge.

In addition to intraspinal injection, median nerve ablation is an additional potential procedure. This procedure is currently commonly performed with computed tomography (CT) guidance, and accuracy in both the orientation and positioning of the tools are critical to a successful outcome for patients [2]. The developed VR system and MRI guided robot are expected to enable the performance of this procedure under MRI guidance, by providing a more intuitive visualization of the target trajectory.

A. MRI Visualization in Virtual Reality

Various MRI rendering solutions have been developed, many tailored to a particular area of interest. Recent work has shown operator viewpoint to be an important factor in surgical task completion times [6]. Augmented and virtual reality are growing areas of research with an expanding body of prior work [7], [8], [9], [10], [11], [12]. In short, the data is combined into a 3D volume, which can then be rendered using various methods of volume rendering to merge points into a surface. Depending on the volume of interest and the data required, many techniques can be used. In this work, the DICOM data is parsed into a three dimensional image, which is then rendered via ray tracing, with optimizations that cause minimal effects to the rendered image. This procedure is performed twice, once per eye, to give the user the perception of depth, making VR more advantageous than traditional methods. There are other programs using similar techniques [10]; however, they were found to be incompatible with the robot configuration and kinematic calculations necessary for this project. Once the rendering solution is established, an additional critical component is the material segmentation. There have been many works relating to segmentation within MRI scans [13], [14], with varying degrees of complexity. VR provides a unique ability for users to be able to intuitively perceive the depth within the MRI scan, as well as freely manipulate the model in six degrees of freedom (DOF). This greatly improves the speed of the targeting process when compared to traditional computer monitor based solutions.

B. MRI Robot Operation

An earlier version of the robotic device utilized in this work was previously described [4], [5] and shown in Figure 1. The robot consists of a parallel plane design by which

W. Meinhold, H. Nieves-Vazquez, D. Martinez, and J. Ueda are with the Woodruff School of Mechanical Engineering, Georgia Institute of Technology, Atlanta, GA

J. Lee, S. Li, and A.-P. Hu, are with the Intelligent Sustainable Technologies Division, Georgia Tech Research Institute, Atlanta, GA.

the planar x-y locations of two ball joints are independently controlled. A guide channel is passed between the ball joints, enabling the guide to be positioned and oriented with 4 DOF. Each axis of the 2 ball joints is actuated by a piezoelectric motor with 5μm step size (Linear 6N, PiezoMotor). The robot relies on image-based feedback for position control, with MR contrasting fiducials located on the guide channel as shown in Figure 2. Image Jacobian control is used to position the fiducials within the scanner coordinate frame, thereby defining the robot configuration without an explicit registration step [4].

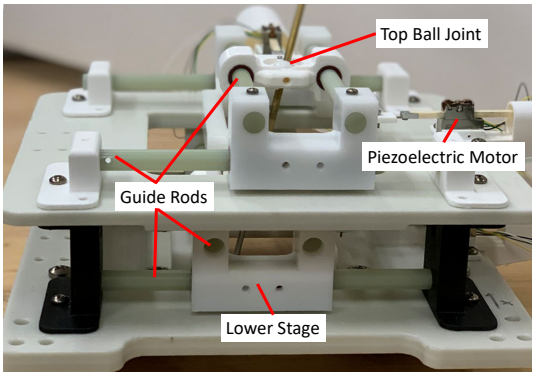

Fig. 1. Robotic guide positioning device

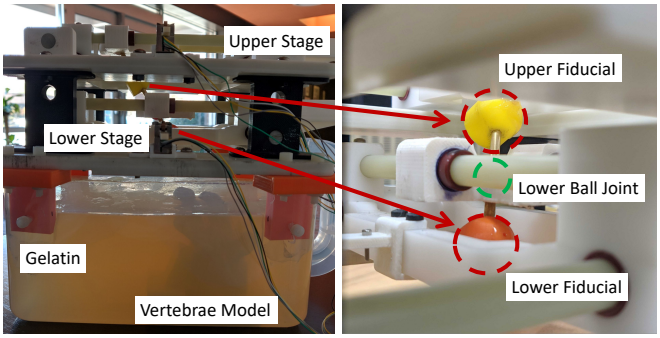

Fig. 2. MRI phantom and contrasting fiducials mounted to the needle guide below each joint

C. Automated Surgical Freedom Analysis

Surgical freedom is a critical factor in choosing the method of approach in anatomically constrained surgical procedures. In the past, most work on this topic has focused on cadeveric studies to compare surgical approaches [15], [16]. While this approach is very useful in the pre-planning of procedures, we hope to leverage this concept to enable faster planning in a VR environment while the robot and patient are in the scanner. The primary application of the MRI guided robotic positioning device is injection, biopsy, and RFA/RFN procedures, all of which predominantly employ straight tools. For this reason, the analysis of surgical freedom presented in this work assumes a straight and rigid tool, with all analyzed trajectories represented by straight lines.

II. Methods

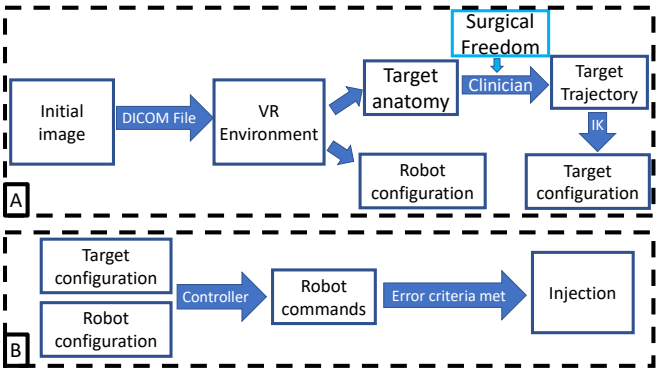

Fig. 3. The VR guided system reported in this work, A) the image guidance system and B) the robot actuation scheme

A. Robotic System

The MRI robot described above was integrated into a VR based navigation system to enable faster and more accurate control and guidance. The system diagram is shown in 2 parts in Figure 3. The robot was designed to forgo traditional position sensors in favor of image guidance. While this is possible to achieve utilizing traditional MR image viewing interfaces [4], two main problems were present in prior works: 1) Estimation of the fiducial locations from the relatively coarse image slice separation and 2) determination of suitable trajectories to avoid obstacles in the anatomy. The implementation of a VR system into the image workflow aids in addressing both of these issues. Images are taken from the scan server as DICOM files, then fiducial locations and the target geometry are automatically assessed and displayed in a VR environment. This key automation step allows rapid and accurate assessment of the robot's current configuration, likely decreasing the number of iterative position updates needed to reach a given target.

The main benefit of performing the image guidance in the VR environment is the ease of visualization. The anatomy around the proposed target injection site, the spine, is both complicated and sensitive to disturbance. It is critical that clinicians are able to clearly and confidently visualize both the target and the robot. Traditional planar projections can allow for detailed inspection of specific anatomical features, but require significant spatial reasoning skill to accurately and reliably interpret and determine needle paths between the vertebrae and into a spinal target. Prior work has found that the performance of clinical radiologists is correlated with spatial reasoning ability [17] for this reason. The VR environment enables clinicians to better understand the anatomy and pick trajectories with confidence.

In addition to the VR environment, this work demonstrates a method for simulating surgical freedom from anatomical models, providing clinicians with an additional layer of information to aid in finding suitable needle trajectories. Once the robot configuration is detected, and the clinician selects a suitable target and needle pose, a target configuration

(fiducial locations) is computed via inverse kinematics. The intersection points of the fiducial planes in the image stack and the target trajectory become the target configuration for the robot.

The goal of any robotic position control scheme is to move from a current configuration to a target configuration. This process is shown in Figure 3B. An image Jacobian method is used recursively, until error reaches a stopping criteria (usually 0 pixels), then the patient and robot can be removed from the scanner and the injection performed.

B. Surgical Freedom

Instead of the cadaver experiments commonly used to evaluate surgical freedom, this work employed a simulation environment. A mesh model of the 3rd lumbar vertebrae was generated, and used as the basis for surgical freedom estimation. The model used was from an open source medical image database [18]. All potential (straight line) trajectories to reach a set target without obstruction by the vertebrae that fit within a 60 degree insertion angle were evaluated numerically. Surgical freedom was then estimated as the relative number of viable trajectories to reach the target. This was measured as a percentage of the available trajectories fitting within the region formed by a 60 degree insertion angle above the vertebrae (targeting the ventral horn from below the patient is not feasible). The simulation of trajectories was done via the COMSOL ray optics module.

C. Virtual Reality System

The VR system developed as part of this work is integrated into the existing MRI guided robotic device workflow. After an initial image is taken in the scanner, the image (in DICOM format) is then loaded into the VR interface (Unity 3D, Oculus Quest device). Immediately after loading, the image is rendered and the user can begin to interact with the image. For this project, each material type is given an adjustable minimum and maximum intensity, roughly mirroring the Hounsfield units (HU) of a CT scan. The render then uses these thresholds and the materials selected by the user to determine which sections of the volume are rendered. Secondly, a linear coloration transfer function is used to approximately color code each material type based on the aforementioned threshold values. Additionally, to aid in the viewing process, the user is able to 'crop' the volume via a set of sliders which controls the minimum and maximum viewable ranges of the x, y, and z coordinate axis. This can be used to easily view into the inside of a solid volume or a noisy scan where the thresholds are insufficient.

Finally, a 'DICOM mode' can be enabled which removes any material segmentation and coloration displaying the DICOM model in the typical greyscale of MRI scans. This mode used in tandem with the coordinate axis clipping can allow one to easily grasp the model and provide a 1:1 mapping with the traditional images the user may be more attuned to.

The VR image workflow is shown in Figure 4. In the VR environment, the virtual vectors can be manipulated to reach a viable direction of the needle using the hand controllers' grasping functionality. Two movable spheres are used to control the target needle direction as shown in Figure 4D. The red sphere represents the origin of the vector that should be placed to coincide with the target in the DICOM images. The green sphere will then be adjusted to decide the direction of the vector. A blue line will move along with the two spheres representing the desired needle direction. In addition, there will be two transparent spheres in the VR environment representing two fiducial spheres, and a greyscale plane is attached to each of the fiducials as shown inf Figure 4E.

These spheres are automatically placed at the detected fiducial locations. Sphere detection uses a Hough transform to detect circles in three orthogonal planes. Since the fiducial's radius is known, the program will only detect a specific radius of a specific range (5-8 cm) to increase efficiency. Once circles are detected in all 3 planes at the same location in a 3D model, the program will recognize this point as the fiducial center point. From the height of these centers, the robot planes are found. The positions of these spheres can also be adjusted freely by using the controllers' grabbing functionality. The blue cubes represent the target fiducial locations, which are the intersection points of the needle vector and the two planes. This representation also gives a clear view of the differences between the desired needle direction and the robot's fiducial spheres. Once the model has been manipulated to the desire of the user, the intersection points from Figure 4E are output as a set of vectors, shown in Figure 4F.

D. MRI Phantom

A phantom was developed consisting of 10% gelatin and an ABS plastic vertebrae. The phantom is shown in Figure 5. The vertebrae model was 3D printed from a modified version of the third and fourth lumbar vertebrae [18]. A spherical cavity filled with vitamin E was placed in the location of the ventral horn of the spinal cord, creating a MR contrasting target.

Morphological images of this phantom were used in the user study described below.

E. User study

A group of novice and expert users were asked to evaluate the VR interface and guidance system and to attempt target trajectory generation. The user feedback process was determined to be exempt from review by the Georgia Institute of Technology Review Board. A total of eight users were sampled, including two experts with mean experience of 15 years in planning needle insertion trajectory procedures from medical images. The novice users did not have medical imaging experience. The users participated in trajectory planning in the developed virtual reality interface. After attempting to define trajectories, the subjects were given a likert scale questionnaire and asked to assess the usability, intuitiveness and perceived accuracy of the developed system. The usability prompt aimed to assess the ease of use in learning to use the interface. The intuitiveness question aimed to gauge

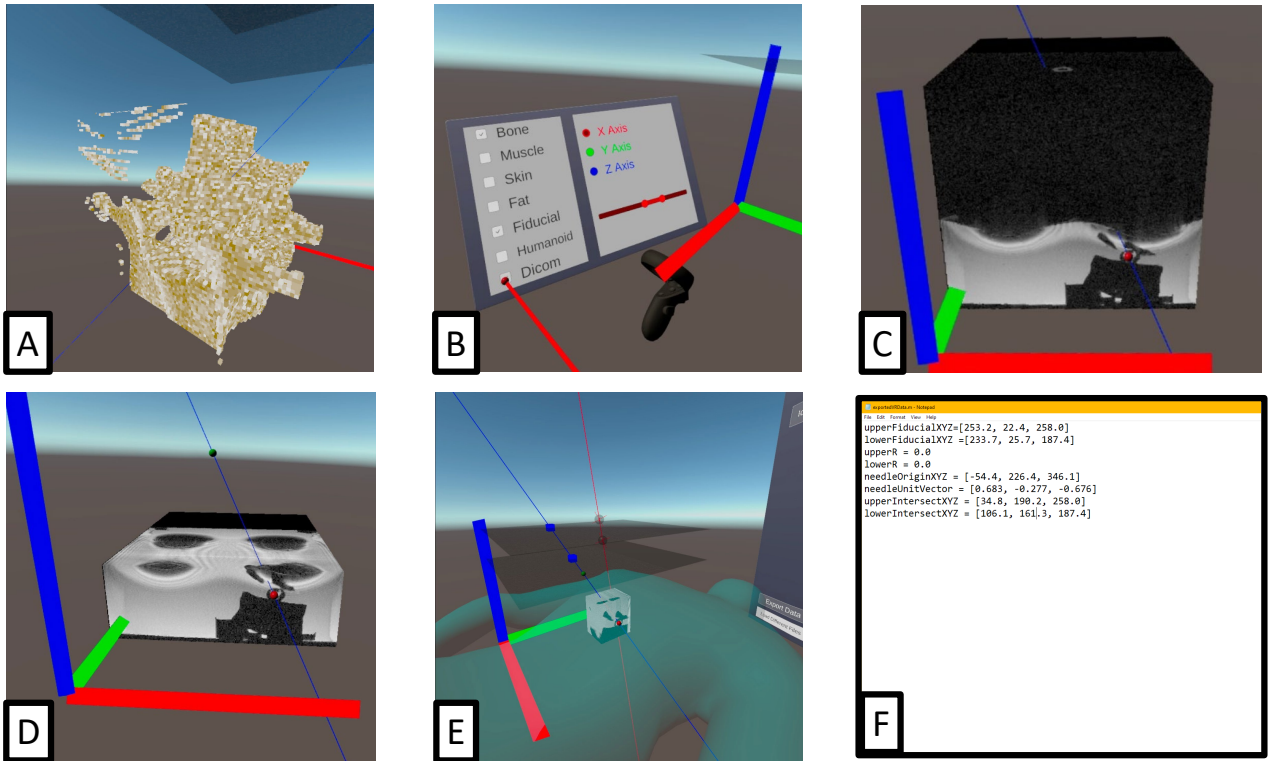

Fig. 4. VR Image processing and procedural steps, A) DICOM data sampled for bone material, B) Material choice and reference frame selection interface, C) Full DICOM image of a gelatin phantom, D) Selected trajectory to the target, E) Detected robot configuration, plane heights and target configuration, F) Program output to controller, current and targeted robot fiducial locations each in Cartesian form

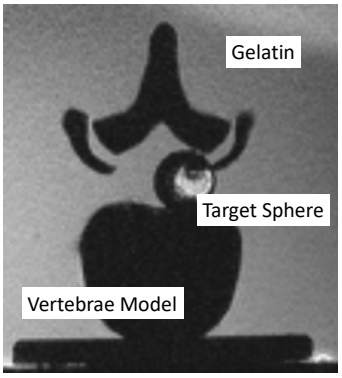

Fig. 5. Axial MRI view of the phantom

the effectiveness of the control layout, while the perceived accuracy question assessed the user's impressions of fidelity in the image rendering and controls. The survey also asked users to compare the system to the one currently used in their clinical practice, where applicable. Novice users reported some familiarity with VR systems (five out of six), along with one of the two experts.

III. Results and Discussion

A. Surgical Freedom Analysis Results

Results from the surgical freedom simulations are shown in Figure 6 and Figure 7. 55940 of the 101500 tested trajectories resulted in a usable needle path, for a surgical freedom of 55.1% in the relevant angular restrictions. Each of the rays in Figure 6 represents a potential trajectory to reach the chosen target in the ventral horn, with the rays stopping at the vertebrae occluded. In Figure 7 the viable trajectories are represented by the blue dots, with the robot positioned above the vertebrae and an example needle path to the target shown in green.

These results provide a useful guide for the user of the VR interface, because the simulation provides an estimate for the regions where target trajectories will be found. The complexity and requirements of the geometric restrictions to the potential trajectories can be increased to account for sensitive soft tissues or other important anatomical features to avoid; however, this work only considered the immediate vertebral obstacle. For a more accurate estimation of the true relative surgical freedom, a more complex model of the spine is necessary, however the basic computational steps are identical to those outlined in Section II-B.

Future work will seek to more tightly integrate the surgical freedom estimation and robot control scheme. However, computation time limits the ability to make such estimations from the MR images directly while the robot is operating in the scanner. From the results presented, clinicians can be given a starting point to reference before exploring patient specific trajectories in the VR environment.

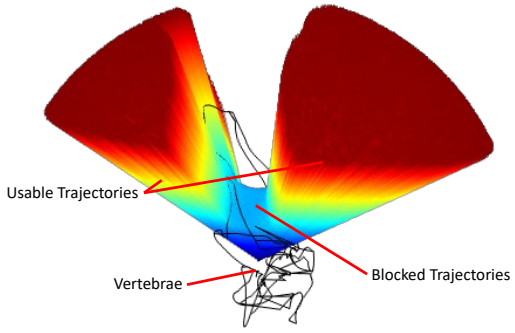

Fig. 6. Surgical freedom simulation results with all potential trajectories shown

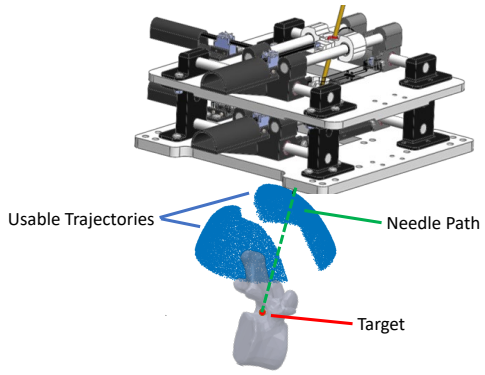

Fig. 7. Surgical freedom simulation results with robot and vertebrae model, an example needle path is shown in green

B. User Study Results

1) Novice Users: The novice user survey results are shown in Table I. Users rated the ease of learning and intuitiveness of the controls quite highly. Perceived accuracy of the system was also moderately high. The intuitive nature of the controls is particularly notable, since users were asked to generate trajectories on a spinal MRI model, which they lacked experience with. It is possible that the immersive nature of the VR environment allows the user to direct attention to manipulation of the controls, rather than visualization or interpretation of a two dimensional image.

TABLE I

MEAN RESULTS OF THE NOVICE USER SURVEY (N = 6), ANSWERS WERE ALL ON A STANDARD LIKERT SCALE ((LOWEST)1-10(HIGHEST))

Attribute	Mean(Std)
Ease of learning the VR interface	8.50 (1.26)
Intuitiveness	8.00 (0.58)
Perceived accuracy of the system	7.75 (1.30)

2) Expert Users: The expert user mean results for each of the survey questions is shown below, in Table II. The results indicate that the experts found the system to be relatively easy to learn, although they ranked it lower than the novices did. They also compared the VR system somewhat unfavorably to current clinical practice and other visualization tools. This low rating should be mitigated by addressing the qualitative feedback explored below.

Both expert users and multiple novice users stated that the slider sensitivity should be reduced, or the length of the slider increased, to allow for easier fine-tuning of the minimum and maximum viewable limits of each axis. One expert suggested setting the blue line of the targeted needle direction to a length that is scaled to the DICOM image, or adding tick marks representing units of length. A scaled needle direction length could aid clinicians in choosing the correct needle depth for a procedure. One expert believed that reducing the viewable limits of the DICOM image to only the target region of the procedure may not be necessary for a single clinician, but could be beneficial when communicating the procedure plan to others. One expert noted the system's potential to assist in planning procedures and both experts suggested broadening the application of the system to include teaching students.

The most important suggestion made by both expert users is enabling diagonal viewing limits of the DICOM image. They stated this could be done if the axes that the sliders adjust along are kept fixed, rather than rotating relative to the DICOM image. This is particularly necessary if the target location of the needle trajectory is not parallel to one of the three planes that the sliders control. Future work will involve implementation of a wider arrange of applications, as well as incorporation of the expert user feedback.

TABLE II

MEAN RESULTS OF THE EXPERT USER SURVEY (N = 2), ANSWERS WERE ALL ON A STANDARD LIKERT SCALE ((LOWEST)1-10(HIGHEST))

Attribute	Mean(Std)
Ease of learning the VR interface	5.5 (0.5)
Intuitiveness	5.5 (0.5)
Perceived accuracy of the system	6.5 (1.5)
Utility compared to 3D slicer	3.0 (1.0)
Utility compared to current practice	4.0 (2.0)

IV. CONCLUSION

This work reported an integrated system for the visualization and control of a precise MRI guided robot for targeted interventions. The VR interface described enables automated detection of the robot's configuration directly from the scan data in addition to an intuitive interface for user visualization of the targeted region. Automated surgical freedom analysis augments trajectory selection by providing a visual aid to users. Both novice and expert users found the system relatively easy to learn and rated the intuitiveness of the controls highly. The methods employed in this paper are not only applicable to the specific robot and anatomy investigated, but could be used in a much wider range of MRI guided surgery applications as well.

ACKNOWLEDGMENT

The authors would like to thank Dr. Vishwadeep Ahluwalia of the GSU/GT Center for Advanced Brain Imaging for essential assistance in carrying out the MRI portions

of this work. The authors would also like to thank Dr. Di Cui of Emory Spine Center for evaluation of the VR system.

This work was funded in part by the Georgia Tech Institute for Robotics and Intelligent Machines under the FY2020 seed grant program, and the National Science Foundation under grant number 1662029.

REFERENCES

[1] J. J. Lamanna, L. N. Urquia, C. V. Hurtig, J. Gutierrez, C. Anderson, P. Piferi, T. Federici, J. N. Oshinski, and N. M. Boulis, "Magnetic resonance imaging-guided transplantation of neural stem cells into the porcine spinal cord," *Stereotactic and functional neurosurgery*, vol. 95, no. 1, pp. 60–68, 2017.

[2] B. J. Schneider, L. Doan, M. K. Maes, K. R. Martinez, A. Gonzalez Cota, N. Bogduk, and S. D. of the Spine Intervention Society, "Systematic review of the effectiveness of lumbar medial branch thermal radiofrequency neurotomy, stratified for diagnostic methods and procedural technique," *Pain Medicine*, vol. 21, no. 6, pp. 1122–1141, 2020.

[3] J. D. Glass, N. M. Boulis, K. Johe, S. B. Rutkove, T. Federici, M. Polak, C. Kelly, and E. L. Feldman, "Lumbar intraspinal injection of neural stem cells in patients with amyotrophic lateral sclerosis: results of a phase i trial in 12 patients," *Stem cells*, vol. 30, no. 6, pp. 1144–1151, 2012.

[4] W. Meinhold, D. E. Martinez, J. N. Oshinski, A.-P. Hu, and J. Ueda, "A direct drive parallel plane piezoelectric needle positioning robot for mri guided intraspinal injection," *IEEE Transactions on Biomedical Engineering*, 2020.

[5] D. E. Martinez, W. Meinhold, J. Oshinski, A.-P. Hu, and J. Ueda, "Super resolution for improved positioning of an mri-guided spinal cellular injection robot," *Journal of Medical Robotics Research*, vol. 6, no. 01n02, 2021.

[6] M. Draelos, B. Keller, C. Toth, A. Kuo, K. Hauser, and J. Izatt, "Teleoperating robots from arbitrary viewpoints in surgical contexts," in *2017 IEEE/RSJ International Conference on Intelligent Robots and Systems (IROS)*. IEEE, 2017, pp. 2549–2555.

[7] G. Vadalà, S. De Salvatore, L. Ambrosio, F. Russo, R. Papalia, and V. Denaro, "Robotic spine surgery and augmented reality systems: a state of the art," *Neurospine*, vol. 17, no. 1, p. 88, 2020.

[8] G. Burström, O. Persson, E. Edström, and A. Elmi-Terander, "Augmented reality navigation in spine surgery: a systematic review," *Acta Neurochirurgica*, vol. 163, no. 3, pp. 843–852, 2021.

[9] D. Duncan, R. Garner, I. Zrantchev, T. Ard, B. Newman, A. Saslow, E. Wanserski, and A. W. Toga, "Using virtual reality to improve performance and user experience in manual correction of mri segmentation errors by non-experts," *Journal of digital imaging*, vol. 32, no. 1, pp. 97–104, 2019.

[10] F.-C. Adochiei, R.-I. Ciucu, I.-R. Adochiei, S. D. Grigorescu, G. C. Seriţan, and M. Casian, "A web platform for rendring and viewing mri volumes using real-time raytracing principles," in *2019 11th International Symposium on Advanced Topics in Electrical Engineering (ATEE)*. IEEE, 2019, pp. 1–4.

[11] B. Keller, M. Draelos, K. Zhou, R. Qian, A. Kuo, G. Konidaris, K. Hauser, and J. Izatt, "Oct guided robotic ophthalmic microsurgery via reinforcement learning from demonstration."

[12] B. Keller, M. Draelos, K. Zhou, R. Qian, A. N. Kuo, G. Konidaris, K. Hauser, and J. A. Izatt, "Optical coherence tomography-guided robotic ophthalmic microsurgery via reinforcement learning from demonstration," *IEEE Transactions on Robotics*, vol. 36, no. 4, pp. 1207–1218, 2020.

[13] J. Kratky and J. Kybic, "Three-dimensional segmentation of bones from ct and mri using fast level sets," in *Medical Imaging 2008: Image Processing*, vol. 6914. International Society for Optics and Photonics, 2008, p. 691447.

[14] J. Korhonen, M. Kapanen, J. Keyriläinen, T. Seppälä, and M. Tenhunen, "A dual model hu conversion from mri intensity values within and outside of bone segment for mri-based radiotherapy treatment planning of prostate cancer," *Medical physics*, vol. 41, no. 1, p. 011704, 2014.

[15] A. M. Elhadi, K. K. Almefty, G. A. Mendes, M. Y. S. Kalani, P. Nakaji, A. Dru, M. C. Preul, and A. S. Little, "Comparison of surgical freedom and area of exposure in three endoscopic transmaxillary approaches to the anterolateral cranial base," *Journal of neurological surgery. Part B, Skull base*, vol. 75, no. 5, p. 346, 2014.

[16] L. Anschuetz, L. Presutti, D. Schneider, A. Yacoub, W. Wimmer, J. Beck, S. Weber, and M. Caversaccio, "Quantitative analysis of surgical freedom and area of exposure in minimal-invasive transcanal approaches to the lateral skull base," *Otology & neurotology*, vol. 39, no. 6, pp. 785–790, 2018.

[17] W. Smoker, K. Berbaum, N. Luebke, and C. Jacoby, "Spatial perception testing in diagnostic radiology," *American journal of roentgenology*, vol. 143, no. 5, pp. 1105–1109, 1984.

[18] N. Mitsuhashi, K. Fujieda, T. Tamura, S. Kawamoto, T. Takagi, and K. Okubo, "Bodyparts3d: 3d structure database for anatomical concepts," *Nucleic acids research*, vol. 37, no. suppl_1, pp. D782–D785, 2009.